Rhinocerotoid fossils of the Linxia Basin in northwestern China as late Cenozoic biostratigraphic markers

Article *in* Palaeogeography Palaeoclimatology Palaeoecology · March 2023

DOI: 10.1016/j.palaeo.2023.111427

CITATIONS
0

READS
54

4 authors, including:

Tao Deng
Chinese Academy of Sciences
256 PUBLICATIONS **5,004** CITATIONS
SEE PROFILE

Xiaokang Lu
Henan University of Tcm
11 PUBLICATIONS **51** CITATIONS
SEE PROFILE

Danhui Sun
Chinese Academy of Sciences
8 PUBLICATIONS **36** CITATIONS
SEE PROFILE

Palaeogeography, Palaeoclimatology, Palaeoecology 614 (2023) 111427

Contents lists available at ScienceDirect

Palaeogeography, Palaeoclimatology, Palaeoecology

journal homepage: www.elsevier.com/locate/palaeo

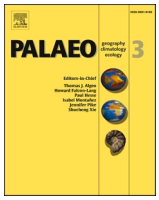

Rhinocerotoid fossils of the Linxia Basin in northwestern China as late Cenozoic biostratigraphic markers

Tao Deng [a,b,c,*], Xiaokang Lu [d], Danhui Sun [a,c], Shijie Li [a,c]

[a] Key Laboratory of Vertebrate Evolution and Human Origins, Institute of Vertebrate Paleontology and Paleoanthropology, Chinese Academy of Sciences, Beijing 100044, China
[b] CAS Center for Excellence in Life and Paleoenvironment, Beijing 100044, China
[c] University of the Chinese Academy of Sciences, Beijing 100049, China
[d] Henan University of Chinese Medicine, Zhengzhou, Henan 450008, China

ARTICLE INFO

Editor: Dr. Howard Falcon-Lang

Keywords:
Rhinocerotoidea
Cenozoic
Biostratigraphy
Paleoecology
Linxia Basin
China

ABSTRACT

This study reports on rhinocerotoid fossils from the Oligocene-Pleistocene strata of the Linxia Basin of Gansu Province, northwestern China. Rhinoceroses have been important components of mammalian faunas of these beds, and include the Late Oligocene giant rhinos (paraceratheres) and the Late Miocene hornless rhinos (aceratheres). As a result of their high diversity, wide geographical distribution and rapid evolution, rhinoceroses are good markers for stratigraphic division and may be used for intercontinental correlations. The Late Oligocene fauna of the Linxia Basin occurs in the lower part of the Jiaozigou Formation. Among 12 species of large mammal fossils, nine are of the superfamily Rhinocerotoidea, and giant rhinos are dominant. Rhinoceroses of the Middle Miocene fauna reflect a forest environment. Comparison with contemporaneous European rhinoceroses suggests a dispersal route for populations along the north side of the Tibetan Plateau. Rhinoceroses were most abundant in the Linxia Basin in the Late Miocene times. The most primitive species of the genus *Chilotherium* and the huge elasmotheres are key indicators for the base of the Upper Miocene (Tortonian). From the Late Miocene to Early Pliocene, the assemblages of the three-toed horse *Hipparion* comprise five horizons, each of which has different rhinocerotid fossils as markers of division and correlation. Because of the strong competition by ruminants, rhinoceroses declined greatly in the Early Pleistocene fauna. At that time, only a species of the woolly rhino persisted, but as an intermediate form, *Coelodonta nihowanensis* of the Linxia Basin can still connect the Pliocene Zanda Basin of the Tibetan Plateau and the Early Pleistocene Nihewan Basin of the North China Plain.

1. Introduction

The Linxia Basin in Gansu Province, northwestern China is rich in late Cenozoic mammalian fossils, including rhinoceros fossils with different horizons, high diversity, and large numbers of individuals (Deng et al., 2004a, 2004b, 2013a; Deng, 2005a). The earliest report of mammalian fossils in this basin was that of Hu (1962), which mainly included the horse *Hipparion* and the rhinoceros *Chilotherium*, the specimens of which were upper and lower jaw fragments with dentition. After a long hiatus, detailed study of the mammalian fossils from the Linxia Basin resumed in the 1980s. Qiu et al. (1988) established the Late Miocene hornless rhino *Acerorhinus hezhengensis*; this species was represented by a complete skull and mandible, collected from the red clay deposits at Dashengou in Hezheng County. Qiu et al. (1990) reported giant rhino fossils in the Linxia Basin and revealed for the first time that there were mammal fossils older than the *Hipparion* fauna in this basin. Qiu and Xie (1998) described the elasmothere fossils in the Linxia Basin, which could be compared with *Parelasmotherium* in the *Hipparion* fauna of Shanxi Province. Since the 2000s, the Hezheng Paleozoological Museum and the Institute of Vertebrate Paleontology and Paleoanthropology of the Chinese Academy of Sciences have collected and stored a large number of rhinoceros fossils from the Linxia Basin (Fig. 1). Deng and others have published a series of new rhinoceros fossil materials, thus establishing the basis of rhinoceros biostratigraphy in the Linxia Basin.

Prior to the 1960s, Cenozoic deposits of the Linxia Basin were simply

* Corresponding author at: Key Laboratory of Vertebrate Evolution and Human Origins, Institute of Vertebrate Paleontology and Paleoanthropology, Chinese Academy of Sciences, Beijing 100044, China.
E-mail address: dengtao@ivpp.ac.cn (T. Deng).

https://doi.org/10.1016/j.palaeo.2023.111427
Received 23 June 2022; Received in revised form 22 January 2023; Accepted 24 January 2023
Available online 30 January 2023

called the Gansu Series. The entire Cenozoic sequence was renamed as the Linxia Formation, subdivided into four members (1 to 4), and regarded as Pliocene based on the *Hipparion* fossils found in the uppermost part of the succession by the local geologic survey team of Gansu Province in 1965. Qiu et al. (1990) created a new formation, the Jiaozigou Formation, in the lower part of the section based on the discovery of a giant rhino-entelodont assemblage, corresponding to members 1 and 2 of the Linxia Fm., thus restricting the Linxia Fm. to members 3 and 4. A research group from Lanzhou University further subdivided the Linxia sequence in the 1990s, nominating a series of new lithological units and dating them mainly using paleomagnetic data (Li et al., 1995; Fang et al., 1997, 2003, 2016). Deng et al. (2004a, 2004b, 2013a) revised the lithological succession and adopted the following units: the Oligocene Tala and Jiaozigou formations, the Miocene Shangzhuang, Dongxiang, Hujialiang, and Liushu formations, the Pliocene Hewangjia and Jishi formations, and the Pleistocene Wucheng Fm. (Fig. 2), and reinterpreted paleomagnetic datings of Fang et al. (2003) for each formation and its mammalian fauna. Fang et al. (2016), Zan et al. (2016), Zhang et al. (2019), Sun et al. (2022) and Zheng et al., 2023 further give precise paleomagnetic datings for these faunas.

2. Rhinocerotoid fossils of the Linxia Basin

2.1. Jiaozigou Formation

The Jiaozigou Formation in the Linxia Basin consists of brownish conglomeratic coarse sandstones with large cross-bedding in the lower part and brownish-red silty mudstones with secondary gypsum in the upper part. Rhinocerotoid fossils come from the sandstone in the lower part of this formation (Fig. 2). The fossil localities include Jiaozigou, Tala, Yagou and Wangjiachuan in Dongxiang County (Fig. 1) (Qiu et al., 1990, 2004b, 2004c; Qiu and Wang, 2007; Deng et al., 2021). Among the 12 known large mammals in the Jiaozigou Fm., nine species are rhinocerotoids, thereby being predominant (i.e., 75% of the total). These species include members of Hyracodontidae, Paraceratheriidae, and Rhinocerotidae, with high diversity.

2.1.1. Hyracodontidae

In the Jiaozigou Fm., the Hyracodontidae are represented by isolated teeth and identified as *Ardynia altidentata*, *Ardynia* sp., *Allacerops* sp., and Hyracodontidae gen. et sp. indet., a total of 4 species (Qiu et al., 2004c).

Although *Ardynia altidentata* is small, it is the largest species of the genus *Ardynia*, with 31.7 mm maximum ectoloph length of M2 (Qiu et al., 2004c). The molar crown is high, and the boundary between the crown and the root fluctuates significantly. M2 is higher-than-long, and the crista, which is wider than the metaloph, is strongly developed; the metaloph is reduced, connecting with the ectoloph at its posterior 1/3. The trigonid of the lower molar becomes shorter on the labial side, whereas the talonid becomes longer. The labial groove is located at the anterior 1/3 of the crown base and above the anterior root. The Linxia M2 is almost the same size as the M2 of Ergilin Dzo in Mongolia (Beliajeva, 1952). Aside from the differences in the metaloph and crista, the Linxia specimen is almost completely identical to the Ergilin Dzo M2 in the outline, ectoloph, protoloph and postflexid. The lower teeth of the Linxia specimens are larger than those from Ergilin Dzo.

Qiu et al. (2004c) identified only one m3 of *Ardynia* sp. The trigonid is V-shaped, the para-protolophid is arc-shaped, the metalophid is straight and oblique postero-lingually, and the postero-labial corner of the protoconid is close to a right angle. The talonid is L-shaped and slightly lower than the trigonid; the postero-labial corner of the hypoconid is rounded. Unlike the undulation of *A. altidentata*, the boundary between the crown and root is nearly straight. There are cingula at the antero-labial corner and the posterior margin. The tooth is similar in size and shape to the m3 of the mandibles of both *Parahyracodon mongoliensis* and *P. kazachstanensis* described by Beliajeva (1952). *Parahyracodon* was subsequently referred to *Ardynia* by Radinsky (1967).

Hyracodontidae gen. et sp. indet. is represented only by p3 and p4 (Qiu et al., 2004c). Based on its small size, with a length of about 20 mm for each premolar, and primitive structure, such as an incompletely

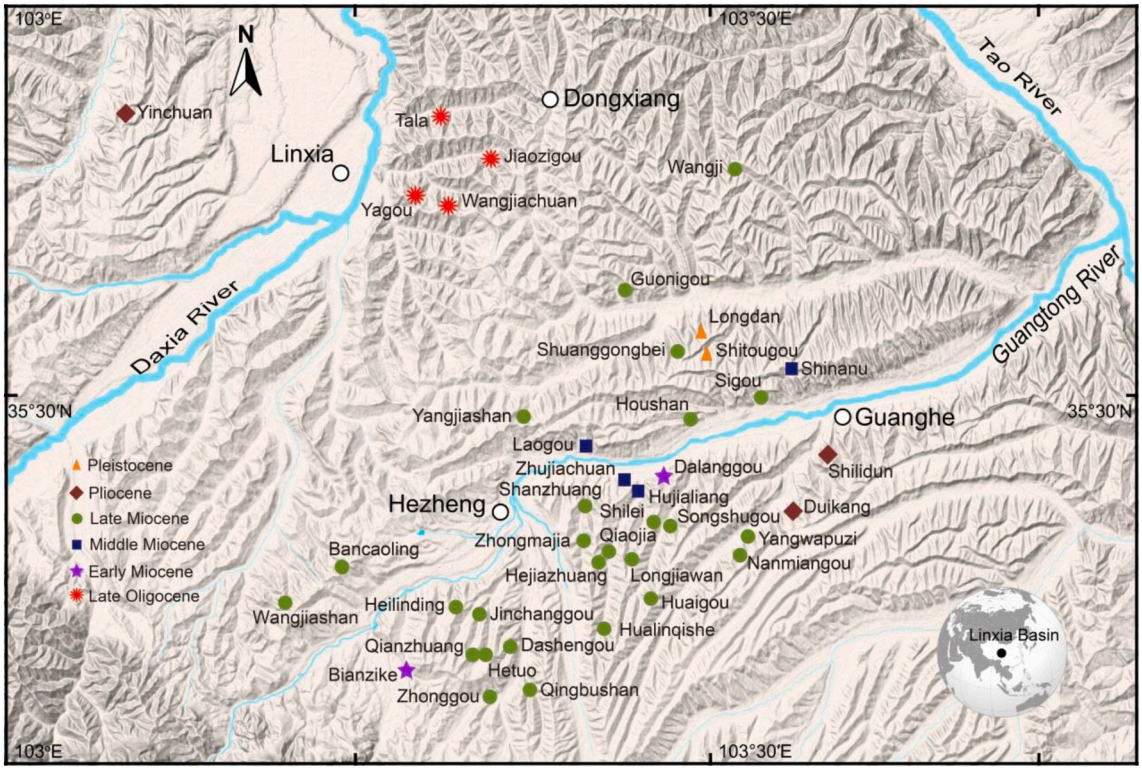

Fig. 1. Topographic map of the Linxia Basin, Gansu Province, China with rhinocerotoid fossil localities.

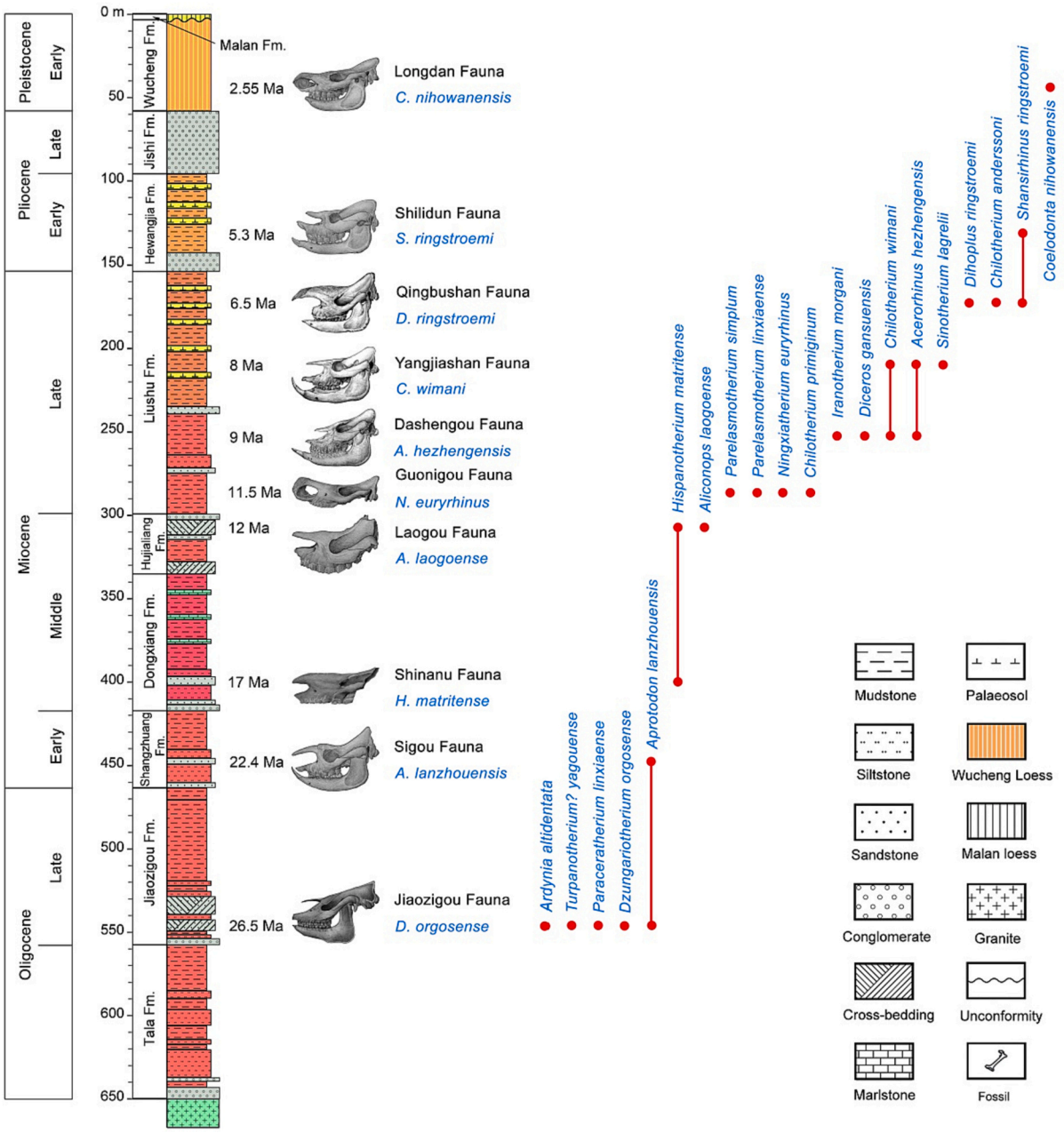

Fig. 2. Stratigraphical section of the Cenozoic deposits of the Linxia Basin with chronostratigraphic range and absolute dates based on Fang et al. (2003, 2016), Deng et al. (2013a), Zan et al. (2016), Zhang et al. (2019), Sun et al. (2022) and Zheng et al., 2023 of rhinocerotoid fossils.

developed hypolophid, it can only be interpreted as a very primitive rhinoceros (Qiu et al., 2004c). These specimens are most similar in shape and size to *Prothyracodon turgaiensis* from Chelkar Teniz, Kazakhstan (Beliajeva, 1954).

2.1.2. Paraceratheriidae

Dzungariotherium orgosense of the Jiaozigou Fm. is represented by many isolated teeth, a broken mandible, and the distal part of a metapodial (Qiu et al., 1990, 2004b; Qiu and Wang, 2007), which are larger than those of *Paraceratherium* and similar to the holotype of *D. orgosense* (Chiu, 1973). The similarities with the holotype on teeth include: P2 is triangular with a front tip; the lingual walls of M2 and M3 are flat with vertical and anterior grooves, the antecrochet is large, and the lingual cingulum is present; the ectometaloph of M3 is round without angular protrusion; in the lower cheek teeth, the cingula are developed and the entoconid is slightly conical. The difference between the Linxia specimen and the holotype of *D. orgosense* is that the teeth of the former are narrower; however, the individual sizes of the giant rhino vary greatly within the same species (Gromova, 1959).

Fossils of *Turpanotherium*? *yagouense* include a juvenile skull of the holotype (Fig. 3A) and isolated left and right M3. It is a small giant rhino, similar in size to *Paraceratherium bugtiense*. The muzzle retracts, and its length does not exceed the length of DP1-DP4, without upper incisors and canines. The upper cheek teeth are high-crowned and covered with thin cement on the labial wall. M1 is high and close to its maximum length, and the lingual wall of the protocone is flat with a vertical groove. The upper deciduous premolars (except DP1) and molars have large antecrochet, the bases of which block the median valley. The protocone has an anterior groove, and the hypocone has a deep one. The anterior and posterior cingula are high-ridged, and the lingual cingulum is absent. There are pillars in the middle of the anterior cingulum, the rear end of the antecrochet, and the entrances of the posterior and

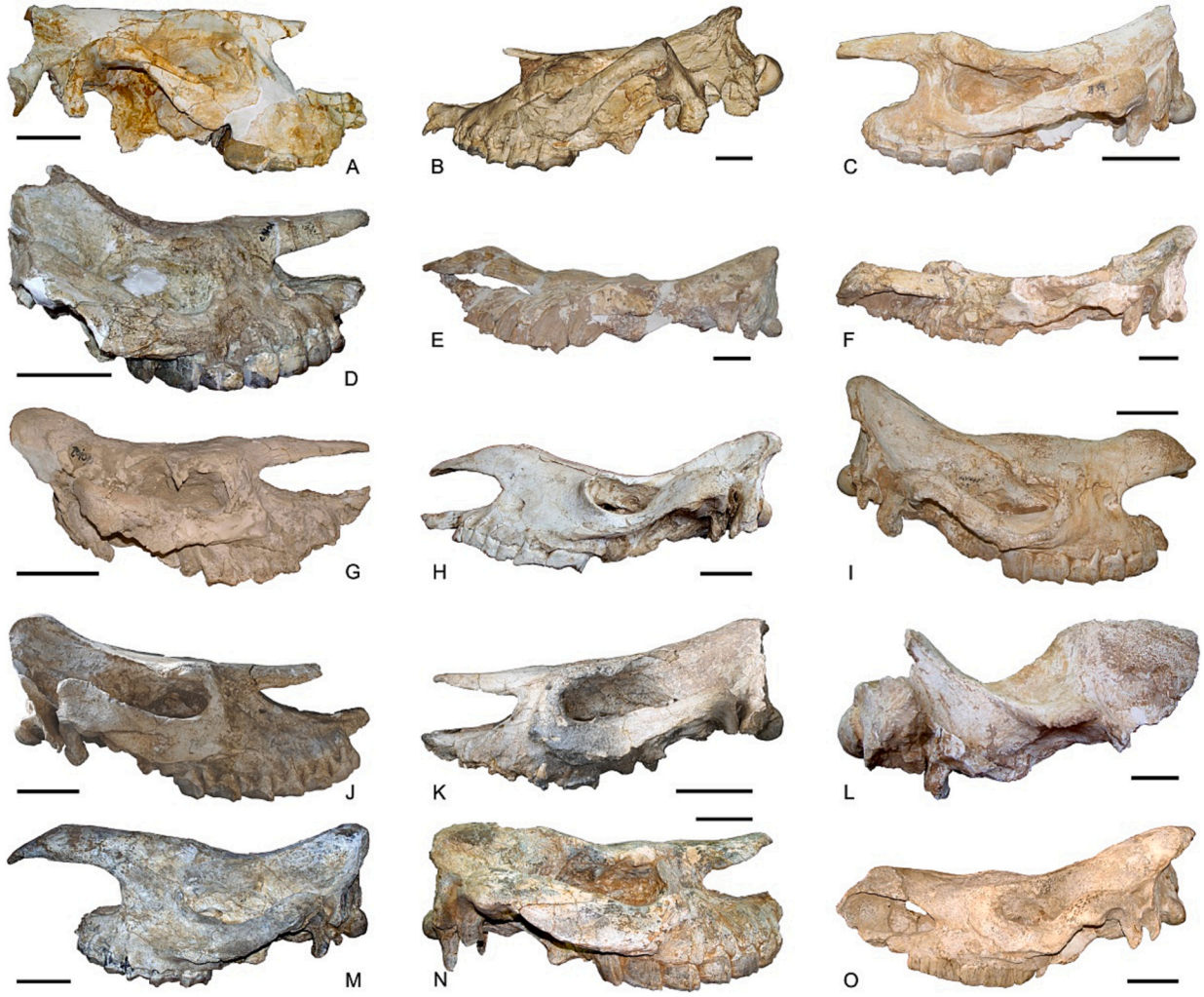

Fig. 3. Rhinocerotoid skulls of the Linxia Basin in lateral view. A. *Turpanotherium yagouense* (IVPP V 13820); B. *Paraceratherium linxiaense* (HMV 2006); C. *Aprotodon lanzhouensis* (IVPP V 13852); D. *Alicornops laogouense* (HMV 0982); E. *Parelasmotherium linxiaense* (HMV 1411); F. *Ningxiatherium euryrhinus* (HMV 1449); G. *Chilotherium primigenius* (HMV 0102); H. *Iranotherium morgani* (HMV 1098); I. *Diceros gansuensis* (HMV 1446); J. *Acerorhinus hezhengensis* (HMV 0639); K. *Chilotherium wimani* (IVPP V 14966); L. *Sinotherium lagrelii* (IVPP V 18539); M. *Dicerorhinus ringstroemi* (HMV 1115); N. *Shansirhinus ringstroemi* (HMV 13764); O. *Coelodonta nihowanensis* (HMV 0980). Scale bars = 10 cm.

median valleys (Qiu et al., 2004b; Qiu and Wang, 2007).

Paraceratherium linxiaense was discovered at Wangjiachuan in Dongxiang County, including a complete skull and mandible (Fig. 3B, 4A) with the associated atlas, as well as an axis and two thoracic vertebrae of a different individual. *P. linxiaense* possesses features that characterize the genus, such as a giant body size, long premaxillae with anterior ends extending downward, separated parietal crests, high condyles compared with the height of the nuchal surface, an inferior border of the posttympanic process lower than the condyle, a roughly horizontal anterior part of the symphysis, and a pair of downward turning cone-shaped I1. It is more derived than other species within this genus in having a larger body size, a deeper nasal notch above M2, a much higher occipital part and posterior end of the zygomatic arch, and a pair of smaller I1. The lower margin of the horizontal mandibular ramus is concave under the diastema, and a pair of small i1 extends anteriorly and horizontally. The dental formula is 1.0.3.3/1.0.3.3. P2 is semimolarized, whereas P3 and P4 are submolarized. The metaconule connects with the ectoloph and the anterior point of the hypocone with moderate wear; the antecrochet is moderate; the lingual border of the protocone is rounded on the molars; and the ecto-posterior corner of the protolophid is angular on p3 and p4. The atlas has an expanded transverse foramen and a dumb-bell shaped vertebral fossa (Deng et al., 2021).

2.1.3. Rhinocerotidae

The materials of *Aprotodon lanzhouensis* from Yagou include a complete skull with its mandible (Fig. 3C, 4B) and an isolated right i2 (Qiu et al., 2004c). Their sizes and shapes are very similar to those of *A. lanzhouensis* from the Lanzhou Basin (Qiu and Xie, 1997). The angle between the anterior and lateral surfaces of the lower incisor is close to a right angle, and the wear surface of the lingual side is very long, extending to the base of the crown, which suggests that *A. lanzhouensis* from the Linxia Basin is female, and *Aprotodon* has significant sexual differences at this point. In addition, the nasal bone of the Linxia specimen is thicker than that of the Lanzhou one.

Ronzotherium has only an isolated left m3, which is relatively primitive in morphology. Its paralophid is short, the postero-labial corner of the protoconid is nearly a right angle, and the hypolophid is reduced (Qiu et al., 1990).

2.2. Shangzhuang Formation

The Shangzhuang Formation consists of yellowish brown carbonate-cemented medium sandstone and brownish red silty mudstones. Only

Fig. 4. Rhinocerotoid mandibles of the Linxia Basin in occlusal view. A. *Paraceratherium linxiaense* (HMV 2006); B. *Aprotodon lanzhouensis* (IVPP V 13852); C. *Chilotherium primigenius* (HMV 0102); D. *Iranotherium morgani* (HMV 1099); E. *Acerorhinus hezhengensis* (HMV 0639); F. *Diceros gansuensis* (HMV 1448); G. *Dicerorhinus ringstroemi* (HMV 2048); H. *Chilotherium wimani* (IVPP V 14966); I. *Shansirhinus ringstroemi* (HMV 13764); J. *Coelodonta nihowanensis* (HMV 0980). Scale bars = 10 cm.

Aprotodon lanzhouensis was discovered from the red silty mudstones of the Shangzhuang Fm. at Dalanggou in Guanghe County and at Bianzike in Hezheng County (Figs. 1, 2), including isolated lower incisors and cheek teeth (Deng, 2006b, 2013). In the lower premolars from Dalanggou, the paralophid is tiny, and the protolophid stretches antero-lingually; the metaconid is robust, slanting postero-lingually; the entolophid is complete, but still very thin. In the lower molars, the labial valley is deep, and the anterior valley is U-shaped, with a rather right-angled posterior end. The lower incisors from Bianzike have a strong curvature and an enamel-free wear facet that is longer than the root, and their roots have a laterally compressed and inferiorly rounded cross section. Very thin enamel covers the anterior and labial surfaces with numerous black longitudinal cracks. The cross section of the crown is triangular, with sharp antero-lingual and postero-labial angles, a rounded antero-labial angle, a smooth or slightly concave anterior surface, and a slightly convex labial surface.

2.3. Dongxiang Formation

The Dongxiang Formation consists of brownish sandstones, purplish red mudstones and siltstones intercalated with a number of bluish grey or grayish white marlite beds of 0.5–1 m thick. Fossils of the *Anchitherium* fauna, including the elasmothere *Hispanotherium matritense* and the acerathere *Alicornops* sp., were found in the lower sandstone of the Dongxiang Fm. at Shinanu in Guanghe County (Figs. 1, 2). All of these fossils are isolated teeth (Deng et al., 2004b).

2.4. Hujialiang Formation

The Hujialiang Formation consists of brownish or grayish sandstones and conglomerates. The fossils of *Hispanotherium matritense* from the Hujialiang Fm., mainly collected at Laogou in Hezheng County (Figs. 1, 2), include many isolated teeth and some broken mandibles. They are generally similar to specimens from other localities in Eurasia, with minor differences (Deng, 2003). The upper cheek teeth have an undulating labial border of the ectoloph, variable enamel folds in the median valley, and a well-defined boundary between the ectoloph and metaloph of M3. The lower cheek teeth have a high crown and a marked constriction groove of the metaconid, and m3 is narrow.

The material of *Alicornops laogouense* from the Hujialiang Fm. includes an adult skull without the occipital surface (Fig. 3D) and some isolated teeth. The skull is high and mid-sized, about 30% smaller than that of the extant *Rhinoceros unicornis*, but larger than other known species of the genus *Alicornops* (*A. simorrense* and *A. alfambrense*). There is no horn on the nasals or the frontal. It differs from *A. simorrense* in the following ways: the nasals are 1.7 times as long as wide, but the width of the nasal base is narrower; the skull is much higher; the skull roof is lozenge-shaped, with a narrower maximal frontal width; the frontal bone narrows posteriorly, but less strongly; the surface between the parietal crests is slightly wider with a minimum width of 25 mm; the nasal notch is situated at the level of the middle of P3, shallower than that of *A. simorrense* at the level of P4; the postorbital process is much weaker; the anterior margin of the orbit is situated at the level of the anterior part of M1, more anterior than that of *A. simorrense* at the level of the M1/M2 boundary or the anterior part of M2 (Deng, 2004).

2.5. Liushu Formation

The Liushu Formation consists of light yellowish brown carbonate-cemented siltstones (red clays) intercalated with a few thin beds of mudstones and marls, developing substantial mottles and big carbonate nodules. Toward the southern Linxia Basin, more conglomerates are intercalated in the Liushu Fm. The mammal fossils in the Liushu Fm. are very rich, and all belong to the *Hipparion* fauna, which can be divided into four horizons, represented by the localities of Guonigou, Dashengou, Yangjiashan, and Qingbushan in the Linxia Basin (Figs. 1, 2).

2.5.1. Lower horizon

The material of *Parelasmotherium simplum* was collected from Wangji in Dongxiang County, including M1 and M2 (Qiu and Xie, 1998). The

crista is short and small, not or weakly forked at its end; the cristella and postcrista are in initial stage of development, and the enamel is smooth, with almost no secondary plication. The labial half of the anterior cingulum is situated rather high, and the lingual half descends steeply to fuse with the protocone close to the crown base; the posterior cingulum is also situated rather high; the lingual and labial cingula are absent. The posterior valley is triangular. The labial wall shows a weak waveform. The protocone is antero-posteriorly long, with deep contraction before and after, and the antecrochet is large. The paracone of M1 is quite prominent, and the lingual half of the protoloph is obviously oblique backward; the connection of the metaloph with the ectoloph is thin, gradually widening lingually, and the anterior contraction of the hypocone is shallow and wide. The metastyle of M2 is obviously warped labially, and the protoloph is curved posteriorly; the metaloph is thinner than the protoloph; the crochet is absent. The teeth are hypsodont with cement filling in valleys and circumferential covering. M2 erupted much later than M1; that is, M2 did not erupt until M1 was worn to about half. The teeth are the broadest at their bases and longest at the middle of the crown height. The unique prism part of the later elasmotheres has not been differentiated from the crown part of *P. simplum* (Ringström, 1924).

Parelasmotherium linxiaense was found from the bottom of the Liushu Fm. at Guonigou in Dongxiang County, including a skull (Fig. 3E) and isolated teeth (Deng, 2001c, 2007). It is a large elasmothere, and its skull is dolichocephalic. M3 is located in front of the orbit. The nasal horn boss is rough and large, whereas the frontal horn is absent; the nasals are inclined ventrally at anterior half, and the nasal notch is deep; the premaxillary is narrow and long, without incisors; the lower rim of the orbit is raised; the skull roof is concave, with broadly separated parietal crests; the nuchal tuberosity is strong. Cheek teeth are hypsodont, with wrinkled enamel, well-developed crista, and an expanded hypocone.

Another complete elasmothere skull was discovered from the same layer as *P. linxiaense* at Guonigou, and was established as *Ningxiatherium euryrhinus* (Fig. 3F) (Deng, 2008a). It is also a large elasmothere. Its M3 is located in front of the orbit. The nasals are very wide, with a ventrally inclined anterior part and a thick ossified septum; the terminal nasal horn boss is rough and large, whereas the frontal horn is absent; the nasal notch is situated above the P3/P4 boundary; the premaxillae are narrow and long, and are fused with each other, without incisors; the anterior and lower rims of the orbit are raised; the skull roof is shallowly concave, with a high occipital elevation and broadly separated parietal crests; the occipital surface is vertical. Cheek teeth are extremely hypsodont, with wrinkled enamel, short premolars, a closed posterior valley, and a weak or absent parastyle. These character states are considered derived within rhinocerotids.

At Zhongmajia in Hezheng County, a skull with associated its mandible was collected from the sandstone and conglomerate at the bottom of the Liushu Fm. (Figs. 1, 2); these bones belonged to *Chilotherium primigenius* (Deng, 2006a). The symphysis is very wide, with a flat ventral surface, different from the concave surfaces of other known *Chilotherium* species; the lower incisors i2 are very large and nearly vertically upturned (Fig. 4C); the parietal crests are very slightly separated, forming a sagittal crest different from the broadly separated parietal crests of *C. anderssoni* and *C. habereri*, and also different from the slightly separated parietal crests lacking a sagittal crest of *C. xizangensis* and *C. wimani*.

2.5.2. Middle horizon

There are a large number of fossil sites for this horizon of the Linxia Basin, and rhinocerotids are the most abundant group at each site. Among them, *Chilotherium wimani* is absolutely dominant; *Acerorhinus hezhengensis*, and *Iranotherium morgani* and *Diceros gansuensis* are occasionally found.

Over one thousand skulls, mandibles, and postcranial bones of *Chilotherium wimani* have been discovered across many localities in the middle and upper parts of the Liushu Fm. in Hezheng, Guanghe, and Dongxiang counties (Figs. 1, 2) (Deng, 2001a; Liang and Deng, 2005; Chen et al., 2010). *C. wimani* is mid-sized with a basal cranial length of about 530 mm (Deng, 2001b). The occipital surface is higher-than-wide, and the occipital crest bears a wide median notch. The orbit is large and in a comparatively low position, with strong supraorbital tubercles, weak postorbital processes on the frontal and zygomatic bones, and irregular infraorbital foramina (Fig. 3K). The skull has a narrow and long rhombic dorsal outline, a concave dorsal profile, hardly separated parietal crests, and steep outer walls of the braincase. The nasals are wide and separated from the maxillary bones by a deep nasal notch. Its particularly wide mandibular symphysis has concave dorsal and ventral surfaces, and its large i2 has an upturned medial flange (Fig. 4H). The premolars have well-developed lingual cingula, parastyle folds and paracone ribs, as well as weakly constricted protocones and hypocones. The fore and hind feet of *C. wimani* are tridactyl (Deng, 2002a), and the limb bones are as short and robust as those of *C. anderssoni* from Baode (Ringström, 1924).

Acerorhinus hezhengensis has also been discovered from the middle and upper parts of the Liushu Fm. at many localities in the Linxia Basin, but the number of individual specimens is much fewer than that of *C. wimani* specimens. The holotype of *A. hezhengensis* was collected from Dashengou in Hezheng County (Qiu et al., 1988). It has a large size with a basal length of about 500 mm. Its posttympanic process is long and strongly compressed latero-medially, and stretches downward beyond the condyles. The pseudoauditory meatus is not closed, or only weakly closed (Fig. 3J). The sagittal crest is absent, and the area bordered by the parietal crests is wide and flat, different from the sagittal crest of *A. zernowi* (Borissiak, 1914, 1915) and the narrow area of *A. fuguensis* (Deng, 2000). The nasal notch is deeply incised above M1, deeper than the shallow notch above P4 in *A. palaeosinensis* (Ringström, 1924), and the orbit is situated comparatively low. The medifossettes are absent in the upper premolars but well-developed in *A. palaeosinensis*. The upper molars have strong protocone constrictions and antecrochets, in contrast to the relative weakness of these features in *A. zernowi*, and the labial walls are undulating, with prominent paracone ribs and parastyle folds. The mandibular symphysis is not widened, but ascends anteriorly (Fig. 4E).

The specimens of *Iranotherium morgani* include a complete young male skull and an adult mandible missing the ascending ramus from Houshan, and a complete adult female skull from Shanzhuang, both in Guanghe County (Fig. 1) (Deng, 2005c). These specimens are generally similar to the skull and mandible of *I. morgani* from Maragha, Iran (de Mecquenem, 1908), with minor differences. *I. morgani* is a large elasmothere with a very large nasal horn; its skull is particularly elongate and dorsally concave, with a basilar length of 775 mm; the parietal crests are broadly separate; the nasals are long and wide, with a shallow nasal notch; the orbit is prominent, with the anterior margin situated at level of M3 (Fig. 3H). The skull of *I. morgani* has distinct sexual dimorphism: the nasal horn of the male is much larger than that of the female, and a strong and rough hemispherical hypertrophy is present on the posterior part of the male's zygomatic arch, which is uplifted and higher than the skull roof. The paroccipital process is completely fused with the posttympanic process. The teeth are hypsodont, covered and filled with cement, and the enamel is slightly wrinkled. The premolars are significantly shortened. A marked difference between the specimens from Linxia and Maragha exists in the length ratio of the lower premolars to molars. Because p2 strongly overlaps with p3, which also markedly overlaps with p4, the premolar row on the Linxia mandible is very short (Fig. 4D), with a ratio of 0.4, compared with 0.6 for the mandible from Iran. We propose that this difference is because of individual or sexual variations.

The holotype and other skulls and mandibles of *Diceros gansuensis* came from Houshan (Fig. 1) (Deng and Qiu, 2007). This species is a mid-sized rhinocerotine with a basal skull length of about 620 mm, smaller than that of *D. neumayri* with a basal length of 690 mm (Antoine and Saraç, 2005). The skull is brachycephalic, and the premaxillae are reduced and edentulous. The nasal notch is above the P3/P4 boundary

(Fig. 3I), deeper than that of the living black rhino *D. bicornis* above the P2/P3 boundary. The dorsal cranial profile is concave. The occipital elevation is higher than that of *D. neumayri*, and the occipital surface is vertical, narrow and high; the maximum occipital width is at the base, and the occipital crest is shallowly concave, whereas it is deeply concave in *D. neumayri*. The paroccipital process is short and small, and the sagittal keel and tubercle on the basioccipital are strong. The mandibular symphysis is narrow, the horizontal ramus is thick, and the ascending ramus is vertical and thin, with a short distance to m3 (Fig. 4F). The premolars are comparatively small, the crista is weak, and the antecrochet is absent; the metaloph is absent on DP1, whereas it is present on that of *D. neumayri*; the protoloph is isolated on P2, and the metaloph is narrow on P2 and P3.

2.5.3. Upper horizon

At this horizon of the Liushu Fm., the aceratheres *Acerorhinus hezhengensis* and *Chilotherium wimani* continued to flourish in many localities, and the elasmothere *Sinotherium lagrelli* first appeared at one site.

A partially preserved skull of *Sinotherium lagrelii* was collected from Huaigou in Guanghe County (Fig. 1) (Deng et al., 2013b). The maxillary surface before the orbit is high, vertical, smooth and flat, identical to the unique features of this area of *S. lagrelii* from Baode, Shanxi (Ringström, 1924). The posterior part of the nasals is strongly swollen, with a large, rough area for horns. The dorsal profile of the skull is strongly concave, the posterior part of the zygomatic arch is low, the occiput is so highly elevated that the parietal bones form a very steep surface (Fig. 3L), and the parietal crests are broadly separated. The occipital condyles are transversely very wide. The postglenoid process is robust, and the posttympanic process is laterally expanded; the two processes are not fused with each other. The foramen magnum is very large, elliptical, and higher-than-wide. The occipital condyles are very large, indicating that the connection with the neck was very powerful to support the weight of a dolichocephalic head with two large horns.

2.5.4. Top horizon

Some localities near the southern border of the Linxia Basin and at the top of the Liushu Fm., such as Qingbushan, Wangjiashan, Jinchanggou, and Bancaoling in Hezheng County (Figs. 1, 2), have produced the aceratheres *Chilotherium anderssoni* and *Shansirhinus ringstroemi*, as well as the rhinocerotine *Dihoplus ringstroemi* (Ringström, 1924; Deng, 2006b; Deng et al., 2013a).

The upper cheek teeth of *C. anderssoni* show advanced characters that distinguish them from those of *C. wimani*, such as a flat labial wall almost without a paracone rib and a parastyle fold, the absence of the medifossette, a strongly constricted protocone, and a robust antecrochet. In the upper premolars of *C. anderssoni*, the lingual cingulum is weak and discontinuous, whereas in the upper molars, the lingual cingulum and the crista are completely absent, and the antecrochet is large enough to fill in almost the entire median valley.

Several skulls of the rhinocerotine *Dihoplus ringstroemi* were discovered from the uppermost red clay of the Liushu Fm. This species is dolichocephalic, with a very wide infraorbital foramen on each maxillary. The nasals are long and wide, with a large and domed horn boss. The nasal notch is widely U-shaped in lateral view, and it ends at the level of the P3/P4 boundary. The anterior margin of the orbit is located at the level of the middle of M2. The occiput is not notably raised (Fig. 3M). The frontal horn boss is small, and the parietal crests are broadly separated. The posttympanic and the postglenoid processes are fused with each other. The antecrochet is absent in the premolars, and the protocone is not constricted.

2.6. Hewangjia Formation

The Hewangjia Formation consists of yellowish brown calcareous mudstones encompassing big carbonate nodules intercalated by many calcareous beds, with basal sandstones or conglomerates. The representative fossil localities of the Hewangjia Fm., Shilidun and Duikang in Guanghe County, and Yinchuan in Jishishan County (Figs. 1, 2), bear fossils of *Shansirhinus ringstroemi* (Deng, 2005b; Deng et al., 2011a). The premaxillae of *S. ringstroemi* are significantly retracted and lack upper incisors. The nasals are short and risen, with a rough horn boss on the tip (Fig. 3N). The mandibular symphysis is moderately expanded (Fig. 4I), with a concave labial surface. DP1 is very small. The protocone is strongly constricted. The bridge and medifossette are well-developed on the premolars, with elaborate enamel plications and a continuous lingual cingulum. The trigonid is angularly U-shaped. The skull from Yinchuan resembles that of *S. ringstroemi* from Huangshigou in Yushe, Shanxi (Ringström, 1927; Kretzoi, 1942), with respect to the maxillary and dental morphologies. Similarities include a narrow choana, a widely arched palate, and a relatively prominent anterior end of the zygomatic arch. The teeth are characterized by rich enamel plications, a weak parastyle fold, relatively small DP1, a very strong crochet, and a strongly constricted protocone. The premolars have a well-developed lingual bridge, a strong medifossette, an angularly U-shaped lingual valley, a continuous lingual cingulum, and a squarely expanded hypocone. Differences also exist between the specimens from Yinchuan and Huangshigou. On the premolars of the latter, there are two or three medifossettes, the lingual bridge is strong, and the lingual pillar is absent on P3. These differences represent individual variations within the species (Deng, 2005b). The dental characteristics of specimens from the Hewangjia Fm. are different from numerous and long enamel plications, and lacking the strongly bifurcated or trifurcated crochet of *S. brancoi* from China (Schlosser, 1903; Kretzoi, 1942).

2.7. Wucheng Formation

The Wucheng Formation consists of yellowish hard loess with layers of calcite concretions. The rhinocerotid fossils from the Wucheng Fm. have been identified as *Coelodonta nihowanensis*, and include a skull with its mandible of medium age, a middle part of skull of juvenile age, and limb bones from Longdan in Dongxiang County (Figs. 1, 2) (Deng, 2002b, 2006b, 2008b; Qiu et al., 2004a). This species is morphologically more primitive than *C. antiquitatis*, but more derived than *C. thibetana* (Deng et al., 2011b). Its skull is not particularly elongate, with a basilar length of about 650 mm, shorter than those of *C. antiquitatis* and *C. thibetana*. The facial part is relatively short, and the anterior end of the nasal bones is separated from the premaxillary. The preorbital bar is very short, and the anterior border of the orbit is located anterior to M3. The zygomatic arch is curved (Fig. 3O). The sagittal surface between the parietal crests is narrow, with the narrowest part about 50 mm wide. The opisthion does not extend very strongly backwards. The ascending ramus of the mandible is not strongly slanted backwards. The alveoli of the lower incisors are present. The cement covering is very thin. The premolars, especially p2, remain relatively large (Fig. 4J). The protocone in the upper cheek teeth is not strongly slanted backwards, and the postfossette in P2-P4 formed later in ontogeny. M3 is triangular in form, the same as in *C. thibetana*, whereas it is rectangular in *C. antiquitatis*. The postero-labial corner of the protoconid in the lower cheek teeth is blunt, and the meta- and ento-conids are not clearly swollen (Qiu et al., 2004a).

3. Rhinocerotoid biostratigraphy in the Linxia Basin

Rhinocerotoid fossils are very rich in the Linxia Basin, and appear in every mammalian fossil horizon (Fig. 2). In the Jiaozigou Formation, perissodactyl fossils have an absolute advantage, and their main representatives are rhinoceroses, including members of the Hyracodontidae, Paraceratheriidae, and Rhinocerotidae, which have the highest diversity at the family level. In the overlying Shangzhuang Fm., the abundance and diversity of rhinoceros fossils sharply decreased: the Hyracodontidae and Paraceratheriidae disappeared completely, and only one species of the Rhinocerotidae was found. After that, the Linxia Basin became an

ecosystem dominated by the Rhinocerotidae. The compositions of rhinocerotid fossils in the Dongxiang and Hujialiang formations are similar; there are only two species, and their individual numbers are far lower than that of proboscideans in the fauna at the same time. The rhinocerotids of the Liushu Fm. were the most prosperous in terms of diversity and population number, including four acerathere species, five elasmothere species, and two rhinocerotine species. Rhinoceroses replaced *Hipparion* as the dominant group in the Old World and North America at the same time, and *Chilotherium* became the dominant form in the fauna. In the Hewangjia Fm., *Chilotherium* had disappeared, and only one acerathere species, *Shansirhinus ringstroemi* was present, which subsequently went completely extinct. *Coelodonta nihowanensis*, a descendant of the Pliocene *C. thibetana* of the Tibetan Plateau, has been found in the Wucheng Fm., and it is the last known representative of rhinoceros fossils in the Linxia Basin.

3.1. Jiaozigou Fauna

The Jiaozigou Fauna comes from the lower sandstones of the Jiaozigou Formation (Deng et al., 2021) with the first appearances of *Paraceratherium linxiaense*, *Turpanotherium yagouense*, and *Ardynia altidentata* as well as the last appearance of *Dzungariotherium orgosense*. The holotype of *D. orgosense* was found in the brown layer of the Manas Group of the Junggar Basin in Xinjiang Province, and its age is Late Oligocene (Chiu, 1973). The *D. orgosense* fossils found in the Linxia Basin show that the geological age of the giant rhino fauna is likely Late Oligocene. Cladistic analysis indicated that the clade consisting of *P. linxiaense* and *P. lepidum* is the sister group of *P. bugtiense* (Deng et al., 2021). *P. bugtiense* was recorded from the Oligocene Bugti Member of the lower Chitarwata Fm. in Pakistan (Antoine et al., 2003; Métais et al., 2009; Welcomme et al., 2001), and *P. lepidum* appears in the top horizon of the Late Oligocene Hetaoyuanzi Fm. of the Turpan Basin in Xinjiang (Xu and Wang, 1978) and Late Oligocene deposits in Atasui, central Kazakhstan (Lucas and Bayshashov, 1996). *Turpanotherium elegans*, in the same genus as *T. yagouense*, was also collected from the top of the Hetaoyuanzi Fm. (Qiu and Wang, 2007).

In terms of shape and size, the lower premolars of the Hyracondontidae gen. et sp. indet. are most similar to those of *Prothyracodon turgaiensis* found in the Early Oligocene strata containing giant rhino fossils in Chelkar Teniz, Kazakhstan (Beliajeva, 1954), but the latter is slightly smaller and likely slightly older. *Ardynia* sp. is similar to "*Parahyracodon*" in Ergilin Dzo (latest Eocene) and Chelkar Teniz (Early Oligocene). *Ardynia altidentata* is significantly more advanced in structure and larger than the type species *A. praecox* from the Late Eocene. *A. altidentata* is more advanced than the Early Oligocene "*Parahyracodon*"; therefore, it may be a Late Oligocene species. *Aprotodon lanzhouensis* is mainly found in the Oligocene strata, but also in Early Miocene strata (at the bottom of the middle member of the Xianshuihe Fm. in the Lanzhou Basin; Qiu and Xie, 1997).

A paleomagnetic dating at Yagou indicates that the Jiaozigou Fauna is collected from the lower part of the Jiaozigou Fm. at C9n with the age of 26.5 Ma (Sun et al., 2022). In summary, the geological age of the Jiaozigou Fauna is determined as Late Oligocene.

3.2. Sigou Fauna

The Sigou Fauna is represented by small mammalian fossils in the Shangzhuang Formation at Sigou in Guanghe County (Qiu et al., 2023) with the last appearance of *Aprotodon lanzhouensis*. Teeth of *A. lanzhouensis* occur in the same layer at Dalanggou in Guanghe County (Deng, 2006b) and Bianzike in Hezheng County (Deng, 2013), and are similar to teeth of this species from the Early Miocene white sandstone of the Xianshuihe Fm. in the adjacent Lanzhou Basin (Qiu and Xie, 1997). There is no direct paleomagnetic dating at Sigou, Dalanggou, and Bianzike, but the correlation to the magnetostratigraphy of the Magou and Yagou sections can give an estimated age of about 22.4 Ma within C6B for the Sigou Fauna (Sun et al., 2022; Zheng et al., 2023).

3.3. Shinanu Fauna

The Shinanu Fauna was found from the lower part of the Dongxiang Formation at Shinanu in Guanghe County (Qiu et al., 2023) with the first appearance of *Hispanotherium matritense*. *H. matritense* is a characteristic species of MN 4–5 in Europe (Iñigo and Cerdeño, 1997), and appears in the Lengshuigou Fm. in Lintong, Shaanxi (Zhai, 1978); the Shaping Fm. in Fangxian, Hubei (Yan, 1979); Lower Youshashan Fm. in Delingha, Qinghai (Deng and Wang, 2004); the middle part of the Zhangenbao Fm. in Tongxin, Ningxia (Guan, 1993); and the lower part of the Tunggur Fm. in Sonid Left Banner, Inner Mongolia, with an age of early Tunggurian (Deng et al., 2007). In contrast, *H. matritense* from Shinanu is significantly smaller than *H. tungurense* in the upper part of the Tunggur Fm. (Cerdeño, 1996). *Alicornops* sp. is also found in the lower part of the Dongxiang Fm. at Dalanggou in Guanghe County. In Europe, *Alicornops* first appeared in MN 3 of Wintershof-West, Germany (Ginsburg and Guérin, 1979), was widely distributed in MN 6 of Europe (Heissig, 1999; Cerdeño and Sànchez, 2000), and also found in the Middle Miocene of Turkey (Heissig, 1976). Therefore, based on rhinocerotid fossils, the age of the Shinanu Fauna is likely early Middle Miocene; that is, early Tunggurian.

According to the paleomagnetic datings at the Maogou, Mansancun, and Niujiacun sections, the lower sandstone of Dongxiang Fm. has an age of 17 Ma at C5Cr (Sun et al., 2022).

3.4. Laogou Fauna

The Laogou Fauna was collected from the sandstones of the Hujialiang Formations (Deng et al., 2013a) with the first appearance of *Alicornops simorrense*. Compared with the Middle Miocene *A. simorrense* originating in MN 6 in Europe (Guérin, 1980; Cerdeño and Nieto, 1995; Codrea, 1992, 1996; Lungu, 1984; Kubiak, 1981), *A. laogouense* from the Hujialiang Fm. at Laogou in Hezheng County is larger in size. Therefore, it likely indicates a late Middle Miocene age; that is, the late Tunggurian. The genus *Alicornops* dispersed from Western through Eastern Europe, to western and southern Asia, and to the Far East (Deng, 2004). In the Maogou section, a paleomagnetic dating indicates that the Hujialiang Fm. deposited during 12.8–11.6 Ma (between C5Ar.2n and C5r.2n) (Zheng et al., 2023).

3.5. Guonigou Fauna

The Guonigou Fauna was collected from the bottom of the Liushu Formation (Deng et al., 2013b) with the first appearances of *Parelasmotherium simplum*, *P. linxiaense*, *Ningxiatherium euryrhinus*, and *Chilotherium primigenius* (Qiu and Xie, 1998; Deng, 2001c, 2006a, 2007, 2008a). According to phylogenetic analysis, *Parelamotherium* is the sister group of the clade consisting of *Sinotherium* and *Elasmotherium* (Sun et al., 2021). *Parelamotherium* is clearly more primitive than *Sinotherium* in having a smaller body size and lower crown, the crown does not have a differentiated prism, and secondary folds are very weak, unlike those of *Sinotherium* and *Elasmotherium*. *Sinotherium* was found in the late Late Miocene Baode Fm. in Baode, Shanxi (Ringström, 1923, 1924), and *Elasmotherium* is mainly distributed in Quaternary deposits; its earliest representative, *E. primigenium*, is from the latest Miocene in Dingbian, Shaanxi (Sun et al., 2021). Therefore, the age of the more primitive *P. simplum* and *P. linxiaense* is likely early Late Miocene.

N. euryrhinus is more primitive than *N. longirhinus* from the Late Miocene in Zhongning, Ningxia (Chen, 1977) in having a subquadrangular M3, a shallower nasal notch, and the presence of DP1 in adults, which are plesiomorphic characters in rhinocerotid evolution (Prothero et al., 1986; Cerdeño, 1995; Antoine, 2002).

C. primigenius is interpreted as the most primitive species of *Chilotherium* described thus far, because some apomorphic characters of the

other *Chilotherium* species are absent in *C. primigenius*: thick posttympanic processes, obviously separated parietal crests, a wide nasal notch, a long distance between the bases of i2 and p2, and a concave ventral surface of the mandibular symphysis (Deng, 2006a). *Chilotherium* is a typical representative of the Late Miocene mammalian fauna in Eurasia. It was widely distributed from the middle and late Bahean onward. *C. primigenius*, as its ancestral type, must have occurred earlier.

In the Guonigou section, *Parelasmotherium linxiaense* and *Ningxiatherium euryrhinus* appeared with the earliest *Hipparion*, *H. dongxiangense* at 11.5 Ma close to the base of C5r.2n (Fang et al., 2016).

3.6. Dashengou Fauna

The Dashengou Fauna was collected from the middle part of the Liushu Formation (Deng et al., 2013b) with the first appearances of *Chilotherium wimani*, *Acerorhinus hezhengensis*, *Iranotherium morgani*, and *Diceros gansuensis*. *C. wimani* is the most abundant species in the Dashengou Fauna, and its phylogenetic position is between those of *C. primigenius* and *C. anderssoni*. The biostratigraphic distributions of the latter species are the early Bahean of the earliest Late Miocene and the Baodean of the latest Miocene, respectively; therefore, *C. wimani* represent a middle to late Bahean age. *C. wimani* was also found in the Lamagou Fauna of middle to late Bahean age in Fugu, Shaanxi (Ringström, 1924; Xue et al., 1995; Qiu et al., 2013).

A. hezhengensis is phylogenetically positioned between *A. tsaidamensis* and *A. palaoesinensis*, based on the flattened labial wall of the upper cheek teeth and the plane between parietal crests (Qiu et al., 1988). In the genus *Acerorhinus*, *A. zernowi* is the most primitive species, with uncontracted protocone and hypocone, and an obvious sagittal crest, and occurred during the Tunggurian of the Middle Miocene in Inner Mongolia (Cerdeño, 1996). *A. tsaidamensis* is characterized by the enlarged antecrochet as well as the contracted protocone and hypocone, and occurred during the early Bahean in the Qaidam Basin of Qinghai Province (Bohlin, 1937; Deng and Wang, 2004). *A. palaeosinensis* is a relatively derived species, which is manifested in its shortened skull, anteriorly positioned nasal notch, and horizontally extended lower incisors; this species occurred during the Baodean in Shanxi Province (Ringström, 1924). Therefore, the age of *A. hezhengensis* is inferred as middle and late Bahean of the early Late Miocene.

Previously, *I. morgani* was discovered only in Maragha and Kerjavol in Iran (Antoine, 2002). In Maragha, *I. morgani* belongs to the middle local biozones of the Maragha Fauna, accompanying *Hipparion prostylum* (Bernor et al., 1996). Mein (1990) and Steininger et al. (1990) correlated the middle Maragha Fauna to the late early and middle Turolian (late MN 11 and early MN 12), between 9.3 Ma and 7.75 Ma. Bernor et al. (1996) suggested that the Maragha faunal sequence correlates with basal MN 11 to middle MN 12, ca. 9 to 7.6 Ma, and that *I. morgani* may have first appeared in MN 11. This shows that *I. morgani* is a biostratigraphic marker of the Late Miocene.

D. gansuensis is more derived than *Paradiceros* in Africa, which is reflected in its deeper nasal notch above the P3/P4 boundary, whereas that of *Paradiceros* is at the P2 level. In *D. gansuensis*, the postglenoid and posttympanic processes are fused rather than separated, the crown is higher, the protocone is not constricted, the antecrochet is absent, and the occlusal outline of M3 is triangular rather than approximately quadrilateral. These derived characters indicate that the age of this species must be later than the Middle Miocene age of *Paradiceros* (Hooijer, 1968; Guérin, 1976). However, *D. gansuensis* is more primitive than *D. neumayri* of the late Late Miocene, that is, the Turolian in Eurasia (Heissig, 1999; Antoine and Saraç, 2005); the former is characterized by a smaller and shorter skull, an undeveloped median groove of the occipital crest, and relatively small premolars. Given the evolutionary position of *D. gansuensis* between *Paradiceros* and *D. neumayri*, its age is inferred to be early Late Miocene.

According to the reinterpretation to the paleomagnetic measurements of Fang et al. (2003), the Dashengou Fauna is within C4A, with an age of about 9 Ma (Deng et al., 2013b).

3.7. Yangjiashan Fauna

The Yangjiashan Fauna was collected from the upper part of the Liushu Formation (Deng et al., 2013b) with the first appearance of *Sinotherium lagrelii*. *Chilotherium wimani* and *Acerorhinus hezhengensis* continued to dominate in this fauna. Previously, *S. lagrelii* was only found in the Baodean deposits in Shanxi Province, indicating that it is a typical Late Miocene member. According to the reinterpretation to the paleomagnetic measurements of Fang et al. (2003), the Yangjiashan Fauna is within C4n.2n, with an age of about 8 Ma (Deng et al., 2013b).

3.8. Qingbushan Fauna

The Qingbushan Fauna was found from the top of the Liushu Formation (Deng et al., 2013b) with the first appearances of *Chilotherium anderssoni*, *Dihoplus ringstroemi*, and *Shansirhinus ringstroemi*. In Baode, Shanxi, *C. anderssoni* was found in Loc. 30 (Daijiagou = T'ai-chia-kou, Ringström, 1924), which is referred to MN 12 (Qiu and Qiu, 1995; Qiu et al., 1999) and correlated with C3Ar and C3Bn, giving it an age range of 6.5–7.0 Ma (Yue et al., 2004). *D. ringstroemi* was discovered in the Baodean *Hipparion* red clay in Xin'an, Henan, and Baode, Shanxi (Ringström, 1924; Arambourg, 1959); the Duodaoshi Fm. in Jingmen, Hubei (Yan, 1979); and the Upper Youshashan Fm. of the Qaidam Basin in Qinghai (Deng and Wang, 2004). Therefore, the two species are typical biostratigraphic markers of the Baodean. The localities with *C. anderssoni* and *D. ringstroemi* are situated in the uppermost red clay of the Liushu Fm. on the southern margin of the Linxia Basin, and their horizon is higher than that of the Yangjiashan Fauna in the central part of the basin; thus, their age is consistent with the Baodean.

S. ringstroemi first appeared in the Late Miocene Mahui Fm. in Yushe, Shanxi and the Late Miocene in Tianzhu, Gansu, and its latest known occurrence was from the Late Pliocene in Yuanmou, Yunnan (Tang et al., 1974; Qiu and Yan, 1982).

According to the reinterpretation to the paleomagnetic measurements of Fang et al. (2003), the Qingbushan Fauna is within C3An.2n, with an age of 6.5 Ma (Deng et al., 2013b).

3.9. Shilidun Fauna

The Shilidun Fauna comes from the bottom of the Hewangjia Formation at Shilidun and Duikang in Guanghe County and Yinchuan in Jishishan County (Deng, 2005b; Deng et al., 2011a, 2013b) with the last appearance of *Shansirhinus ringstroemi*. Similarly, this species was also present in the Early Pliocene Gaozhuang Fm. overlying the Mahui Fm. in the Yushe Basin (Qiu and Yan, 1982; Qiu and Qiu, 1995). Zhang et al. (2019) made a detailed magnetostratigraphic study in the Duikang section, and gave 5.3 Ma at the top of C3r for the *Hipparion* fauna bed bearing *Shansirhinus ringstroemi*.

3.10. Longdan Fauna

The Longdan fauna is present in the lower part of the Wucheng Formation (Qiu et al., 2004a) with the first appearance of *Coelodonta nihowanensis*. *C. nihowanensis* is more primitive than the Middle and Late Pleistocene *C. antiquitatis*; in particular, the posterior half of its nasal septum was not ossified. However, it is more derived than the Pliocene *C. thibetana* from the Zanda Basin in Tibet, in which the posterior 2/3 of the nasal septum was not ossified (Deng et al., 2011b). The holotype of *C. nihowanensis* came from the Early Pleistocene sediments of the Nihewan Basin in Yangyuan, Hebei (Teilhard de Chardin and Piveteau, 1930), and this species was also found in the Early Pleistocene strata of Linyi, Shanxi and Gonghe, Qinghai (Chow and Liu, 1959; Chow and Chow, 1959).

The Matsuyama/Gauss boundary is determined 0.5 m below the

lower fossiliferous bed of the Longdan fauna in the Linxia Basin, whereas the lower boundary of the Reunion subchron is just above the upper fossiliferous bed. This would place this fauna in the 2.55 Ma to 2.16 Ma interval (Qiu et al., 2004c; Zan et al., 2016).

4. Late Cenozoic paleoecology of the Linxia Basin indicated by rhinoceros fossils

Cenozoic climatic changes had great influence on mammalian evolution, and several significant turnovers of mammalian faunas occurred in Eurasia, such as the "Mongolian Remodeling" in the Paleogene (Meng and McKenna, 1998) and the true horse arrival in the Quaternary (Lindsay et al., 1980).

The Linxia Basin is located at the northeast margin of the Tibetan Plateau. The strong uplift of the Tibetan Plateau in the late Cenozoic would inevitably have a great impact on the climate and environment of the Linxia Basin. Fossil pollen analysis indicated that a forest environment existed in the Linxia Basin before the Late Miocene, with tropical and subtropical plants in the Middle Miocene, but that the environment turned to grassland in the Late Miocene, when xeric and sub-xeric grasses greatly increased in abundance and became dominated (Ma et al., 1998). This newly available biome had a profound influence on the evolution and distribution of ungulates (MacFadden, 1992). Mammals are extremely sensitive to changes in the climate and environment. As an ungulate group, rhinoceroses are clearly an important indicator of the paleoecology of the Linxia Basin.

4.1. Late Oligocene

The Late Oligocene (Tabenbulukian) diversity of mammals in the Linxia Basin was low compared with that of subsequent ages. From the perspective of a single group, however, the Perissodactyla maintained very high diversity, and the Rhinocerotoidea in particular accounted for 75% of the entire large mammals at the species level (Deng et al., 2021). At the family level, the Hyracondontidae were the most abundant and represented by four species. The Paraceratheriidae were the most representative family in this period, and include three species, *Dzungariotherium orgosense*, *Paraceratherium linxiaense*, and *Turpanotherium*? *yagouense*, all of which were giant-sized and among the largest land mammals that ever lived (Prothero et al., 1989; Qiu et al., 2004b; Qiu and Wang, 2007; Deng et al., 2021). The giant body size, long metapodials, and specialized anterior dentition of paraceratheres were suitable for open woodlands under humid or arid climatic conditions, and these rhinoceroses could crop vegetation from tree tops (Lucas and Sobus, 1989; Prothero, 2013). Hyracondonts had low crowns and fed on tender tree leaves. However, the most chracteristic feature of hyracondonts is that they had slender limbs and coordinated body shapes, which were suitable for fast running, similar to horses. This suggests the widespread occurrence of open woodland instead of dense forest during the Late Oligocene in the Linxia Basin, with a mix of woodland and grassland, conducive to the free activities of paraceratheres and hyracondonts. The $\delta^{13}C$ and $\delta^{18}O$ values of bulk enamel samples indicate that these rhinoceroses had pure C_3 diets, suggesting that they occupied relatively open habitats or exhibited migratory behavior (Biasatti et al., 2018).

The mandibular symphysis of *Aprotodon* is very wide, resembling that of the hippopotamus; this taxon indicates an extensive aquatic environment. The cheek teeth of *Aprotodon* are subhypsodont (Qiu and Xie, 1997); therefore it mainly ate leaves and soft twigs. Consequently, *Aprotodon* likely lived in rivers that crossed the otherwise open and dry woodland with low diversity under arid or semiarid conditions, leading to its limited distribution and number of individuals.

4.2. Early Miocene

Many Oligocene species were extinct in the Early Miocene; among the large mammals, only *Aprotodon* survived (Deng, 2006b). At that time, the ecological environment would have been rich in rivers and lakes. However, the fact that few fossils have been found suggests that the biome was not particularly rich in this period. Large mammals such as *Aprotodon* were predominantly herbivores and lacked the threat of carnivores. The climatic and environmental characteristics during the Early Miocene may have been similar to those in the Late Oligocene, but differed from the Middle Miocene dense and humid forests with high diversity.

4.3. Middle Miocene

Hispanotherium has been interpreted to have lived in warm conditions (Cerdeño and Nieto, 1995; Iñigo and Cerdeño, 1997). *Alicornops* lived in an environment with associated lakes and swamps (Guérin, 1980), and its short limb bones and robust metapodials were adapted for life on soft soils, in contrast to the long and straight metapodials of other rhinoceroses (Cerdeño, 1998). Enamel C and O isotope results indicated that *Alicornops* preferred to browse within a relatively humid woodland habitat (Biasatti et al., 2018). *Hispanotherium* and *Alicornops* were widely distributed rhinoceroses in Eurasia, especially *H. matritense*, which appeared from Europe to East Asia (Deng, 2003), indicating that the climate and environmental conditions across Eurasia were very similar under the influence of the Middle Miocene climatic optimum. C isotope results showed almost no variation in $\delta^{13}C$ values for *Alicornops* and *Hispanotherium* during the Middle Miocene, which suggests little or no seasonal variation in their diets (Biasatti et al., 2018).

4.4. Late Miocene

The temperature decreased after the warm period of the Middle Miocene (Zachos et al., 2001). At the beginning of the Late Miocene, there were three elasmothere species with extremely high crowns and large bodies, *Parelasmotherium simplum*, *P. linxiaense* and *Ningxiatherium euryrhinus*, and their specialized dentition was interpreted as an adaptation to an abrasive high-fiber diet (Heissig, 1989; Deng, 2007), suggesting that these rhinoceroses grazed on tough grasses. These mammals were highly suited to the temperate steppe dominated by hard C_3 grasses, replacing *Hispanotherium* with a moderate crown and a medium size during the Tunggurian. Detailed analysis has shown that the three large elasmotheres had different niches and ate different grasses, reducing competition among the same group (Deng, 2007, 2008a). The $\delta^{18}O$ values of *Parelasmotherium* may indicate that this elasmothere lived in a relatively open C_3 grassland or wooded grassland environment. The later *Iranotherium morgani* had typical sexual dimorphism, which is a representative feature of herbivores living on grasslands (Deng, 2005c). Its high $\delta^{18}O$ value may suggest that *Iranotherium* drank in an open environment where $\delta^{18}O$ values were relatively high because of evaporation (Biasatti et al., 2018).

In the Late Miocene, aceratheres were very prosperous, and *Chilotherium wimani* was the dominant species in the fauna, which was characterized by herd life (Deng and Downs, 2002; Liang and Deng, 2005; Chen et al., 2010). Another acerathere, *Acerorhinus hezhengensis*, remained a brush feeder with increasing adaptation toward tough, dry vegetation, whereas *Chilotherium* had a diet rich in grasses based on its dental and limb morphology (Heissig, 1999). Heissig (1989) noted that *Chilotherium* showed no sign of neck bending, as seen in other grazing rhinoceroses. He also noted that because *Chilotherium* had enlarged incisors, as opposed to horns, it must have required horizontal positioning of the head, and therefore could only graze by shortening the limbs to lower the head to the ground. The small $\delta^{13}C$ range suggests that *Chilotherium* was a selective feeder, which is consistent with its specialized dentition and ability to adapt to increasingly arid conditions in the open steppe environment of the Linxia Basin (Biasatti et al., 2018).

The Baodean *Dihoplus ringstroemi* was a large-body-size rhinocerotid with high crowned teeth and cursorial limb bones (Guérin, 1980). Its

habit was very similar to that of the extant *Ceratotherium simum*, adapted for life in a steppe (Ringström, 1924). Heissig (1989) classified *Dihoplus* as a browser, although it had a lowered head and lost incisors. The $\delta^{13}C$ and $\delta^{18}O$ values of *Dihoplus* were very similar to those of *Chilotherium* during the Baodean, suggesting that these two genera had similar diets and habitats. The C and O isotope data do not support the interpretation that *Dihoplus* was a woodland dweller that browsed, but support the inference that this rhinoceros likely grazed on C_3 grasses in an open steppe environment (Biasatti et al., 2018).

An extinction event at the end of the Late Miocene caused a decline in rhinocerotid diversity, and *Shansirhinus ringstroemi* was the only known survivor into the Pliocene in the Linxia Basin and even in China.

4.5. Early Pliocene

The high crown and strong wear of the teeth of *Shansirhinus* imply that it grazed on tough grasses, and the well-developed secondary folds (crochet, antecrochet, crista, medifossette, constricted protocone, and lingual bridge) and enamel plications being efficient means for its teeth to resist the abrasion of a high-fiber diet. Thus we conclude that *Shansirhinus* was a grazer because it has a premolar morphology unique to certain rhinoceroses and horses, such as *Elasmotherium* and *Hipparion* that have the grazing adaptations of high-crowned and strongly plicate teeth, which indicate an open and dry ecological environment (Deng, 2005b).

The $\delta^{13}C$ values of enamel from *S. ringstroemi* indicate that this rhinoceros had a pure C_3 diet similar to those of apparent grazing rhinoceroses that lived during the Miocene in the Linxia Basin, and that was ^{13}C-enriched compared with rhinoceroses thought to have been forest-dwellers. The enamel $\delta^{18}O$ values of *S. ringstroemi* are high, also suggesting that it drank water in an open environment (Biasatti et al., 2018).

4.6. Early Pleistocene

Because the earliest known occurrence of the woolly rhino was in the Zanda Basin in the southwestern Tibetan Plateau at 5.08 Ma (Wang et al., 2013), it is apparent that the woolly rhino evolved in high Tibet and later moved down the mountains and spread into North Asia and Europe as the global climate became cooler (Deng et al., 2011b). The nasal horn boss of the Early Pleistocene *Coelodonta nihowanensis* of the Linxia Basin indicates that the nasal horn of this rhinoceros was already bilaterally flattened, in contrast to the mostly rounded horn cross section of most living rhinoceroses; such flattening would have given this woolly rhino added profile for an increased effective sweeping area. The downwardly curved nasal tip indicates a strongly forward inclined horn, and the posteriorly reclined occiput indicates a habitually low-slung cranial posture for feeding at ground level. Collectively, these cranial features are strong indications of a species adapted for survival in cold, snow-covered terrain (Deng et al., 2011b). *C. nihowanensis* has been interpreted as a grazer based on its dental morphology, and it was smaller and had a more cursorial limb structure than the more derived species of *Coelodonta* (Deng, 2006b, 2008b).

The enamel $\delta^{18}O$ values of *C. nihowanensis* were high, similar to those of *Shansirhinus ringstroemi*, which suggests that both rhinoceroses drank water in similar open environments. However, the O isotope composition of *C. nihowanensis* was slightly less ^{18}O-enriched compared with that of *S. ringstroemi*, which would be expected, as temperatures were cooler during the Early Pleistocene because of Northern Hemisphere glaciation (Biasatti et al., 2018).

5. Conclusions

Members of the Rhinocerotoidea have consistently been found to have been the dominant mammals in the Linxia Basin in the strata deposited continuously from the late Paleogene to the Quaternary. Paraceratheres and hyracodonts were typical elements of the Oligocene fauna, and lived in an open woodland environment. *Aprotodon* occurred through the Oligocene to Early Miocene and was a typical element of the Oligocene-Miocene transition. The *Hispanotherium-Alicornops* assemblage was restricted to the warm and humid Middle Miocene forest. *Ningxiatherium*, *Parelasmotherium*, *Iranotherium*, *Chilotherium*, *Acerorhinus*, and *Dihoplus* appeared beginning in the Late Miocene in an arid steppe environment, and *Chilotherium* was the dominant and most common form in the *Hipparion* fauna. During the Pliocene, only *Shansirhinus* was present. *Coelodonta* was a biostratigraphic marker of the Pleistocene, adapted to a cold climate. Rhinocerotid records in the Linxia Basin are comparable with those of their relatives found in other localities of Eurasia and Africa. Furthermore, highly diverse and abundantly preserved rhinocerotids from the Late Miocene allow us to conclude that the Linxia Basin was the last refuge for rhinoceroses in East Asia, with a hot climate and strong seasonality.

It is clear that from the end of the Paleogene onward, the evolution of rhinocerotoids was driven by adaptation to a progressively open environment, typically reflected by further specialization of the feeding apparatus, including modification of the teeth and the rostral area. We highlighted that elasmotheres combined two aspects and evolved to their most advanced level by the Late Miocene, with hypsodont teeth and large horns. By the Pleistocene, however, elasmotheres and aceratheres could not bear the cooling climate, and *Coelodonta* succeeded in adapting to a cold grassland environment. Enamel isotopic data show that although the open environment gradually dominated the Linxia Basin, C_3 plants remained, and coexisting rhinoceros species would have had distinct feeding preferences and occupied different niches. Overall, the Linxia Basin is in a good position to reveal the evolution of the Rhinocerotoidea and its relation with climate change through the Oligocene to the Quaternary, and to demonstrate the value of this group as ideal biostratigraphic markers.

Author contributions

T.D. designed the study and wrote the paper; all authors reviewed the manuscript.

Declaration of Competing Interest

The authors declare that they have no conflict interests.

Data availability

Data will be made available on request.

Acknowledgements

We thank the Second Comprehensive Scientific Expedition on the Tibetan Plateau for organizing, all members of the Linxia Basin project leaded by Prof. Zhanxiang Qiu for field work and discussion, Dr. Shiqi Wang and Mr. Yu Chen for drawing, Mr. Wei Gao for photographing, and Ms. Sara J. Mason for improving the manuscript. Dr. Lawrence Flynn, Dr. Xiaoming Wang, Dr. Chenglong Deng, Dr. Jinbo Zan, and an anonymous reviewer are kindly acknowledged for their editing and comments on the manuscript. This research was supported by the Chinese Academy of Sciences (QYZDY-SSW-DQC022, XDB26000000, XDA20070203), and the National Natural Science Foundation of China (42172001).

References

Antoine, P.-O., 2002. Phylogénie et évolution des Elasmtheriina (Mammalia, Rhinocerotidae). Mém. Mus. Natl Hist. Nat. 188, 1–359.
Antoine, P.-O., Ducrocq, S., Marivaux, L., Chaimanee, Y., Crochet, J.-Y., Jaeger, J.-J., Welcomme, J.-L., 2003. Early rhinocerotids (Mammalia, Perissodactyla) from South

Asia and a review of the Holarctic Paleogene rhinocerotid record. Can. J. Earth Sci. 40, 365–374.
Antoine, P.-O., Saraç, G., 2005. Rhinocerotidae (Mammalia, Perissodactyla) from the late Miocene of Akkaşdağı, Turkey. Geodiversitas 27, 601–632.
Arambourg, C., 1959. Vertébrés continentaux du Miocène supérieur de l'Afrique du Nord. Publ. Serv. Car. Géol. Algérie Paléont. 4, 1–159.
Beliajeva, E.I., 1952. Primitive rhinocerotoids of Mongolia. Tr Paleont Inst 41, 120–143 (in Russian).
Beliajeva, E.I., 1954. New material of Tertiary rhinocerotoids of Kazakhstan. Tr. Paleont. Inst. 47, 24–54.
Bernor, R.L., Solounias, N., Swisher, C.C.I.I.I., van Couvering, J.A., 1996. The correlation of three classical 'Pikermian' mammal faunas—Maragha, Samos and Pikermi—with the European MN unit system. In: Bernor, R.L., Fahlbusch, V., Mittmann, H.-W. (Eds.), The Evolution of Western Eurasian Neogene Mammal Faunas. Columbia Univ. Press, New York, pp. 137–156.
Biasatti, D., Wang, Y., Deng, T., 2018. Paleoecology of Cenozoic rhinos from Northwest China: a stable isotope perspective. Vert. PalAsiat. 56, 45–68.
Bohlin, B., 1937. Eine Tertiäre Säugetier-Fauna aus Tsaidam. Pal. Sin. N. Ser. C 14 (1), 1–111.
Borissiak, A.A., 1914. In: Mammalian fossils of Sebastopol, I. Tr. Geol. Komiteta N. Ser, 87, pp. 1–154.
Borissiak, A.A., 1915. In: Mammifères fossiles de Sebastopol, II. Tr. Geol. Komiteta N. Ser, 137, pp. 1–45.
Cerdeño, E., 1995. Cladistic analysis of the family Rhinocerotidae. Am. Mus. Novit. 3134, 1–25.
Cerdeño, E., 1996. Rhinocerotidae from the Middle Miocene of the Tunggur Formation, Inner Mongolia (China). Am. Mus. Novit. 3184, 1–43.
Cerdeño, E., 1998. Diversity and evolutionary trends of the family Rhinocerotidae (Perissodactyla). Palaeogeogr. Palaeoclimatol. Palaeoecol. 141, 13–34.
Cerdeño, E., Nieto, M., 1995. Evolution of Rhinocerotidae in Western Europe: influence of climatic changes. Paleogeogr. Paleoclimatol. Paleoecol. 114, 325–338.
Cerdeño, E., Sànchez, B., 2000. Intraspecific variation and evolutionary trends of *Alicornops simorrense* (Rhinocerotidae) in Spain. Zool. Scrip. 29, 275–305.
Chen, G.-F., 1977. A new genus of Iranotheriinae of Ningxia. Vert. PalAsiat. 15, 143–147.
Chen, S.-K., Deng, T., Hou, S.-K., Shi, Q.-Q., Pang, L.-B., 2010. Sexual dimorphism in perissodactyl rhinocerotid *Chilotherium wimani* from the Late Miocene of the Linxia Basin (Gansu, China). Acta Palaeont. Pol. 55, 587–597.
Chiu, C.-S., 1973. A new genus of giant rhinoceros from Oligocene of Dzungaria, Sinkiang. Vert. PalAsiat. 11, 182–191.
Chow, B.-S., Liu, H.-Y., 1959. Some Pleistocene mammalian fossils from Gunghe, Qinhai. Paleovert. Paleoanthrop. 1, 217–223.
Chow, M.-C., Chow, B.-S., 1959. Villafranchian mammals from Lingyi, S. W. Shansi. Acta Palaeontol. Sin. 7, 89–97.
Codrea, V., 1992. New mammal remains from the Sarmatian deposits at Minisu de Sus (Taut, Arad County). Stud. Univ. Babes-Bolyai Geol. 37, 35–41.
Codrea, V., 1996. Miocene rhinoceroses from Romania: an overview. Acta Zool. Cracov. 39, 83–88.
Deng, T., 2000. A new species of *Acerorhinus* (Perissodactyla, Rhinocerotidae) from the Late Miocene in Fugu, Shaanxi,China. Vert. PalAsiat. 38, 203–217.
Deng, T., 2001. Cranial ontogenesis of *Chilotherium wimani* (Perissodactyla, Rhinocerotidae). In: Deng, T., Wang, Y. (Eds.), Proceedings of the Eighth Annual Meeting of the Chinese Society of Vertebrate Paleontology. China Ocean Press, Beijing, pp. 101–112.
Deng, T., 2001b. New materials of *Chilotherium wimani* (Perissodactyla, Rhinocerotidae) from the Late Miocene of Fugu,Shaanxi. Vert. PalAsiat. 39, 129–138.
Deng, T., 2001c. New remains of *Parelasmotherium* (Perissodactyla, Rhinocerotidae) from the Late Miocene in Dongxiang, Gansu, China. Vert. PalAsiat. 39, 306–311.
Deng, T., 2002. Limb bones of *Chilotherium wimani* (Perissodactyla, Rhinocerotidae) from the Late Miocene of the Linxia Basin in Gansu, China. Vert. PalAsiat. 40, 305–316.
Deng, T., 2002. The earliest known wooly rhino discovered in the Linxia Basin, Gansu Province, China. Geol. Bull. China 21, 604–608.
Deng, T., 2003. New material of *Hispanotherium matritense* (Rhinocerotidae, Perissodactyla) from Laogou of Hezheng County (Gansu, China), with special reference to the Chinese Middle Miocene elasmotheres. Geobios 36, 141–150.
Deng, T., 2004. A new species of the rhinoceros *Alicornops* from the Middle Miocene of the Linxia Basin, Gansu, China. Palaeontology 47, 1427–1439.
Deng, T., 2005a. Character, age and ecology of the Hezheng Biota from northwestern China. Acta Geol. Sin. 79, 739–750.
Deng, T., 2005b. New cranial material of *Shansirhinus* (Rhinocerotidae, Perissodactyla) from the lower Pliocene of the Linxia Basin in Gansu, China. Geobios 38, 301–313.
Deng, T., 2005c. New discovery of *Iranotherium morgani* (Perissodactyla, Rhinocerotidae) from the Late Miocene of the Linxia Basin in Gansu, China and its sexual dimorphism. J. Vert. Paleont. 25, 442–450.
Deng, T., 2006a. A primitive species of *Chilotherium* (Perissodactyla, Rhinocerotidae) from the Late Miocene of the Linxia Basin (Gansu, China). Cain. Res. 5, 93–102.
Deng, T., 2006b. Neogene rhinoceroses of the Linxia Basin (Gansu, China). Cour. Forsch. Senckenberg 256, 43–56.
Deng, T., 2007. Skull of *Parelasmotherium* (Perissodactyla, Rhinocerotidae) from the Upper Miocene in the Linxia Basin (Gansu, China). J. Vert. Paleont. 27, 467–475.
Deng, T., 2008a. A new elasmothere (Perissodactyla, Rhinocerotidae) from the Late Miocene of the Linxia Basin in Gansu, China. Geobios 41, 719–728.
Deng, T., 2008b. Comparison between the woolly rhino's forelimbs from Longdan, northwestern China and Tologoi, Transbaikalian region. Quat. Intern. 179, 196–207.
Deng, T., 2013. Incisor fossils of *Aprotodon* (Perissodactyla, Rhinocerotidae) from the Early Miocene Shangzhuang Formation of the Linxia Basin in Gansu, China. Vert. PalAsiat. 51, 131–140.
Deng, T., Downs, W., 2002. Evolution of Chinese Neogene Rhinocerotidae and its response to climatic variations. Acta Geol. Sin. 76, 139–145.
Deng, T., Hou, S.-K., Shi, Q.-Q., Chen, S.-K., He, W., Chen, S.-Q., 2011a. Terrestrial Mio-Pliocene boundary in the Linxia Basin, Gansu, China. Acta Geol. Sin. 85, 452–464.
Deng, T., Hou, S.-K., Wang, H.-J., 2007. The Tunggurian stage of the continental Miocene in China. Acta Geol. Sin. 81, 709–721.
Deng, T., Lu, X.-K., Wang, S.-Q., Flynn, L.J., Sun, D.-H., He, W., Chen, S.-Q., 2021. An Oligocene giant rhino provides insights into *Paraceratherium* evolution. Comm. Biol. 4, 639. https://doi.org/10.1038/s42003-021-02170-6.
Deng, T., Qiu, Z.-X., 2007. First discovery of *Diceros* (Perissodactyla, Rhinocerotidae) in China. Vert. PalAsiat. 45, 287–306.
Deng, T., Qiu, Z.-X., Wang, B.-Y., Wang, X.-M., Hou, S.-K., 2013a. Late Cenozoic biostratigraphy of the Linxia Basin, northwestern China. In: Wang, X.-M., Flynn, L.J., Fortelius, M. (Eds.), Fossil Mammals of Asia: Neogene Biostratigraphy and Chronology. Columbia Univ. Press, New York, pp. 243–273.
Deng, T., Wang, S.-Q., Hou, S.-K., 2013b. A bizarre tandem-horned elasmothere rhino from the late Miocene of northwestern China and origin of the true elasmothere. Chin. Sci. Bull. 58, 1811–1817.
Deng, T., Wang, X.-M., 2004. New material of the Neogene rhinocerotids from the Qaidam Basin in Qinghai,China. Vert. PalAsiat. 42, 216–229.
Deng, T., Wang, X.-M., Fortelius, M., Li, Q., Wang, Y., Tseng, Z.J., Takeuchi, G.T., Saylor, J.E., Säilä, L.K., Xie, G.-P., 2011b. Out of Tibet: Pliocene woolly rhino suggests high-plateau origin of Ice Age megaherbivores. Science 333, 1285–1288.
Deng, T., Wang, X.-M., Ni, X.-J., Liu, L.-P., 2004a. Sequence of the Cenozoic mammalian faunas of the Linxia Basin in Gansu, China. Acta Geol. Sin. 78, 8–14.
Deng, T., Wang, X.-M., Ni, X.-J., Liu, L.-P., Liang, Z., 2004b. Cenozoic stratigraphic sequence of the Linxia Basin in Gansu, China and its evidence from mammal fossils. Vert. PalAsiat. 42, 45–66.
Fang, X.-M., Garzione, C., Van der Voo, R., Li, J.-J., Fan, M.-J., 2003. Flexural subsidence by 29 Ma on the NE edge of Tibet from the magnetostratigraphy of Linxia Basin, China. Earth Planet. Sci. Lett. 210, 545–560.
Fang, X.-M., Li, J.-J., Zhu, J.-J., Chen, H.-L., Cao, J.-X., 1997. Division and age dating of the Cenozoic strata of the Linxia Basin in Gansu, China. Chin. Sci. Bull. 42, 1457–1471.
Fang, X.-M., Wang, J.-Y., Zhang, W.-L., Zan, J.-B., Song, C.-H., Yan, M.-D., Appel, E., Zhang, T., Wu, F.-L., Yang, Y.-S., Lu, Y., 2016. Tectonosedimentary evolution model of an intracontinental flexural (foreland) basin for paleoclimatic research. Glob. Planet. Change 145, 78–97.
Ginsburg, L., Guérin, C., 1979. Sur l'origine et l'extension stratigraphique du petit Rhinocerotide miocene *Aceratherium* (*Alicornops*) *simorrense* (Lartet 1851) nov. subgen. Com. Ren. Som. Soc. Géol. France 3, 114–116.
Gromova, V., 1959. Giant rhinoceroses. Tr. Paleont. Inst. 71, 1–164.
Guan, J., 1993. Primitive elasmotherines from the Middle Miocene, Ningxia (northwestern China). Mem. Beijing Nat. Hist. Mus. 53, 200–207.
Guérin, C., 1976. Les restes de Rhinocéros du gisement miocène de Beni Mellal. Maroc. Géol. Méditerran. 3, 105–108.
Guérin, C., 1980. Les rhinocéros (Mammalia, Perissodactyla) du Miocène terminal au Pleistocène supérieur en Europe occidentale: comparason arec les expèces actuelles. Doc. Lab. Géol. Lyon Sci. Terre 79, 1–1185.
Heissig, K., 1976. Rhinocerotidae (Mammalia) aus der *Anchitherium*-fauna Anatoliens. Geol. Jahrb. 19, 1–121.
Heissig, K., 1989. Rhinocerotidae. In: Prothero, D.R., Schoch, R.M. (Eds.), The Evolution of Perissodactyls. Oxford Univ. Press, New York, pp. 399–417.
Heissig, K., 1999. Family Rhinocerotidae. In: Rössner, G.E., Heissig, K. (Eds.), The Miocene Land Mammals of Europe. Verlag Dr. Friedrich Pfeil, München, pp. 175–188.
Hooijer, D.A., 1968. A rhinoceros from the Late Miocene of Fort Ternan. Zool. Mededel. 43, 77–92.
Hu, C.-K., 1962. Pliocene and Pleistocene mammalian fossils from Kansu. Vert. PalAsiat. 6, 88–108.
Iñigo, C., Cerdeño, E., 1997. The *Hispanotherium matritense* (Rhinocerotidae) from Corcoles (Guadalajara, Spain): its contribution to the systematics of the Miocene Iranotheriina. Geobios 30, 243–266.
Kretzoi, M., 1942. Bemerkungen zum System der nachmiozänen Nashorn-Gattungen. Földt. Közl. 72, 4–12.
Kubiak, H., 1981. Equidae and Rhinocerotidae (Perissodactyla, Mammalia) from the Miocene of Przeworno in Lower Silesia. Acta Geol. Polon. 31, 71–79.
Li, J.-J., et al., 1995. Uplift of Qinghai-Xizang (Tibet) Plateau and Global Change. Lanzhou Univ. Press, Lanzhou.
Liang, Z., Deng, T., 2005. Age structure and habitat of the rhinoceros *Chilotherium* during the Late Miocene in the Linxia Basin, Gansu, China. Vert. PalAsiat 43, 219–230.
Lindsay, E.H., Opdyke, N.D., Johnson, N.D., 1980. Pliocene dispersal of the horse *Equus* and late Cenozoic mammalian dispersal events. Nature 287, 135–138.
Lucas, S.G., Bayshashov, B.U., 1996. The giant rhinoceros *Paraceratherium* from the Late Oligocene at Aktau Mountain, southern Kazakhstan, and its biochrological significance. N. Jb. Geol. Palaont. Mh. 9, 539–548.
Lucas, S.G., Sobus, J., 1989. The systematics of indricotheres. In: Prothero, D.R., Schoch, R.M. (Eds.), The Evolution of Perissodactyls. Oxford Univ. Press, New York, pp. 358–378.
Lungu, A.N., 1984. *Hipparion* Fauna of the Middle Sarmatian in Moldavia. Stiinca, Kisinev.
Ma, Y.-Z., Li, J.-J., Fang, X.-M., 1998. Records of the climatic variation and pollen flora from the red beds at 30.6-5.0 Ma in Linxia district. Chin. Sci. Bull. 43, 301–304.
MacFadden, B.J., 1992. Fossil Horses: Systematics, Paleobiology, and Evolution of the Family Equidae. Cambridge Univ. Press, New York.

de Mecquenem, R., 1908. Contribution à l'étude du gisement de vertébras de Maragha et de ses environs. Ann. Hist. Nat. Paris 1, 27–79.
Mein, P., 1990. Updating of MN zones. In: Lindsay, E., Fahlbusch, V., Mein, P. (Eds.), European Neogene Mammal Chronology. Plenum Press, New York, pp. 73–90.
Meng, J., McKenna, M.C., 1998. Faunal turnovers of palaeogenemammals from the Mongolian Plateau. Nature 394, 364–367.
Métais, G., Antoine, P.-O., Baqri, S.R.H., Crochet, J.-Y., de Franceschi, D., Marivaux, L., Welcomme, J.-L., 2009. Lithofacies, depositional environments, regional biostratigraphy and age of the Chitarwata Formation in the Bugti Hills, Balochistan, Pakistan. J. Asian Earth Sci. 34, 154–167.
Prothero, D.R., 2013. Rhinoceros Giants, the Paleobiology of Indricotheres. Indiana Univ. Press, Bloomington.
Prothero, D.R., Guérin, C., Manning, E., 1989. The history of the Rhinocerotoidea. In: Prothero, D.R., Schoch, R.M. (Eds.), The Evolution of Perissodactyls. Oxford Univ. Press, New York, pp. 321–340.
Prothero, D.R., Manning, E., Hanson, C.B., 1986. The phylogeny of the Rhinocerotoidea (Mammalia, Perissodactyla). Zool. J. Linnean Soc. 87, 341–366.
Qiu, Z.-X., Deng, T., Wang, B.-Y., 2004a. Early Pleistocene mammalian fauna from Longdan, Dongxiang, Gansu, China. Pal. Sin. N. Ser. C 27, 1–198.
Qiu, Z.-X., Qiu, Z.-D., 1995. Chronological sequence and subdivision of Chinese Neogene mammalian faunas. Palaeogeogr. Palaeoclimatol. Palaeoecol. 116, 41–70.
Qiu, Z.-X., Qiu, Z.-D., Deng, T., Li, C.-K., Zhang, Z.-Q., Wang, B.-Y., Wang, X.-M., 2013. Neogene land mammal stages/ages of China: toward the goal to establish an Asian land mammal stage/age scheme. In: Wang, X.-M., Flynn, L.J., Fortelius, M. (Eds.), Fossil Mammals of Asia: Neogene Biostratigraphy and Chronology. Columbia Univ. Press, New York, pp. 29–90.
Qiu, Z.-X., Wang, B.-Y., 2007. Paracerathere fossils of China. Pal. Sin. N. Ser. C 29, 1–396.
Qiu, Z.-X., Wang, B.-Y., Deng, T., 2004b. Indricotheres (Perissodactyla, Mammalia) from Oligocene in Linxia Basin, Gansu, China. Vert. PalAsiat. 42, 177–192.
Qiu, Z.-X., Wang, B.-Y., Deng, T., 2004c. Mammal fossils from Yagou, Linxia Basin, Gansu, and related stratigraphic problems. Vert. PalAsiat. 42, 276–296.
Qiu, Z.-D., Wang, B.-Y., Li, L., 2023. Middle Cenozoic micromammals from Linxia Basin, Gansu, China, and their implications for biostratigraphy. Palaeogeogr. Palaeoclimatol. Palaeoecol.
Qiu, Z.-X., Wu, W.-Y., Qiu, Z.-D., 1999. Miocene mammal faunal sequence of China: palaeozoogeography and Eurasian relationship. In: Rössner, G.E., Heissig, K. (Eds.), The Miocene Land Mammals of Europe. Verlag Dr. Friedrich Pfeil, München, pp. 443–455.
Qiu, Z.-X., Xie, J.-Y., 1997. A new species of *Aprotodon* (Perissodactyla, Rhinocerotidae) from Lanzhou Basin, Gansu, China. Vert. PalAsiat. 35, 250–267.
Qiu, Z.-X., Xie, J.-Y., 1998. Notes on *Parelasmotherium* and *Hipparion* fossils from Wangji, Dongxiang, Gansu. Vert. PalAsiat. 36, 13–23.
Qiu, Z.-X., Xie, J.-Y., Yan, D.-F., 1988. A new chilothere skull from Hezheng, Gansu, China, with special reference to the chinese "*Diceratherium*". Sci. Sin. Ser. B 31, 494–502.
Qiu, Z.-X., Xie, J.-Y., Yan, D.-F., 1990. Discovery of some early Miocene mammalian fossils from Dongxiang, Gansu. Vert. PalAsiat. 28, 9–24.
Qiu, Z.-X., Yan, D.-F., 1982. A horned *Chilotherium* skull from Yushe, Shansi. Vert. PalAsiat. 20, 122–132.
Radinsky, L.B., 1967. A review of the rhinocerotoid family Hyracodontidae (Perissodactyla). Bull. Am. Mus. Nat. Hist. 136, 1–46.
Ringström, T., 1923. *Sinotherium lagrelii*, a new fossils rhinocerotid from Shansi. Bull. Geol. Surv. China 5, 91–93.
Ringström, T., 1924. Nashorner der *Hipparion*-fauna Nord-Chinas. Pal. Sin. Ser. C 1 (4), 1–159.
Ringström, T., 1927. Über quartäre und jungtertiäre Rhinocerotiden aus China und der Mongolei. Pal. Sin. Ser. C 4 (3), 1–21.
Schlosser, M., 1903. Die fossilen Säugethiere Chinas nebst einer Odontographie der recenten Antilopen. Abh. Kön. Bayer. Akad. Wiss. 22, 1–221.
Steininger, F., Bernor, R.L., Fahlbusch, V., 1990. European Neogene marine/continental chronologic correlations. In: Lindsay, E., Fahlbusch, V., Mein, P. (Eds.), European Neogene Mammal Chronology. Plenum Press, New York, pp. 15–46.
Sun, D.-H., Deng, T., Jiangzuo, Q.-G., 2021. The most primitive *Elasmotherium* (Perissodactyla, Rhinocerotidae) from the Late Miocene of Dingbian, Shaanxi, China. Hist. Biol. https://doi.org/10.1080/08912963.2021.1907368.
Sun, L., Deng, C.-L., Deng, T., Kong, Y.-F., Wu, B.-L., Liu, S.-Z., Li, Q., Liu, G., 2022. Magnetostratigraphy of the Oligocene mammal fauna of the Linxia Basin, northwestern China. Palaeogeogr. Palaeoclimatol. Palaeoecol. https://doi.org/10.1016/j.palaeo.2023.111404.
Tang, Y.-J., You, Y.-Z., Liu, H.-Y., Pan, Y.-R., 1974. New materials of Pliocene mammals from Banguo Basin of Yuanmou, Yunnan and their stratigraphical significance. Vert. PalAsiat. 12, 60–67.
Teilhard de Chardin, P., Piveteau, J., 1930. Les mammifères fossiles de Nihowan (Chine). Ann. Paléont. 19, l-134.
Wang, X.-M., Li, Q., Xie, G.-P., Saylor, J.E., Tseng, Z.J., Takeuchi, G.T., Deng, T., Wang, Y., Hou, S.-K., Zhang, C.-F., Wang, N., Wu, F.-X., 2013. Mio-Pleistocene Zanda Basin biostratigraphy and geochronology, pre-Ice Age fauna, and mammalian evolution in western Himalaya. Palaeogeogr. Palaeoclimatol. Palaeoecol. 374, 81–95.
Welcomme, J.-L., Benammi, M., Crochet, J.-Y., Marivaux, L., Métais, G., Antoine, P.O., Baloch, I., 2001. Himalayan forelands: palaeontological evidence for Oligocene detrital deposits in the Bugti Hills (Balochistan, Pakistan). Geol. Mag. 138, 397–405.
Xu, Y.-X., Wang, J.-W., 1978. New materials of giant rhinoceros. Mem. Inst. Vert. Paleontol. Paleoanthropol. Acad. Sin. 13, 132–140.
Xue, X.-X., Zhang, Y.-X., Yue, L.-P., 1995. Discovery and chronological division of the *Hipparion* fauna in Laogaochuan Village, Fugu County, Shaanxi. Chin. Sci. Bull. 40, 926–929.
Yan, D.-F., 1979. Einige der Fossilen Miozänen Säugetiere der Kreis von Fangxian in Der Provinz Hupei. Vert. PalAsiat. 17, 189–199.
Yue, L.-P., Deng, T., Zhang, Y.-X., Wang, J.-Q., Zhang, R., Yang, L.-R., Heller, F., 2004. Magnetostratigraphy of stratotype section of the Baode Stage. J. Stratigr. 28, 48–51.
Zachos, J., Pagani, M., Sloan, L., Thomas, E., Billups, K., 2001. Trends, rhythms, and aberrations in global climate 65 Ma to present. Science 292, 686–693.
Zan, J.-B., Fang, X.-M., Zhang, W.-L., Yan, M.-D., Zhang, T., 2016. Palaeoenvironmental and chronological constraints on the Early Pleistocene mammal fauna from loess deposits in the Linxia Basin, NE Tibetan Plateau. Quat. Sci. Rev. 148, 234–242.
Zhai, R.-J., 1978. A primitive elasmothere from the Miocene of Lintung. Shensi. Prof. Pap. Stratigr. Palaeont. 7, 122–126.
Zhang, W.-L., Yan, M.-D., Fang, X.-M., Zhang, D.-W., Zhang, T., Zan, J.-B., Song, C.-H., 2019. High-resolution paleomagnetic constraint on the oldest hominoid- fossil-bearing sequence in the Xiaolongtan Basin, southeast margin of the Tibetan Plateau and its geologic implications. Glob. Planet. Change 182, 103001.
Zheng, Y., Qiu, Z.-X., Qiu, Z.-D., Li, L., Wei, X.-H., Zhang, R., Yue, L.-P., Deng, T., 2023. Revised magnetostratigraphy of the Linxia Basin in the northeast Tibetan Plateau, constrained by micromammalian fossils. Palaeogeogr. Palaeoclimatol. Palaeoecol.